Fracture Mechanics of Concrete Structures, de Borst et al (eds) © 2001 Swets & Zeitlinger, Lisse, ISBN 90 2651 825 0

Numerical modeling of environmentally induced deterioration of concrete

S.Grasberger, F.Bangert, D.Kuhl & G.Meschke
Institute for Structural Mechanics, Ruhr-University Bochum, Germany

ABSTRACT: The paper describes numerical models for durability analyses of concrete structures, taking hygrally and chemically induced degradation processes into account. Two particular models are described. As an example for chemically corrosive mechanisms in concrete structures, the material degradation due to calcium leaching and mechanical loading is addressed. The chemo-mechanical deterioration is modeled within the theory of mixtures based on the total porosity generated by mechanical damage and chemical dissolution of the cement matrix. A coupled hygro-mechanical model for concrete is formulated within the framework of thermomechanics of partially saturated porous media in the sense of Biot's theory. The definition of modified effective stresses, based on relations between stress quantities defined on the meso-level to respective homogenized quantities of the macro-level, allows for the description of moisture dependent material properties. This concept is verified by means of experimental data. A 2D simulation of a base restrained shrinkage wall subjected to uniform drying is presented as a representative numerical example.

1 INTRODUCTION

Due to various interacting mechanisms between mechanically and environmentally induced damage processes, coupled analyses are indispensable for reliable predictions of the life-time of concrete structures. Out of the broad spectrum of environmentally induced degradation mechanisms of RC structures, two deterioration mechanisms having completely different origins and different time scales are addressed in this paper: phenomena related to moisture transport and chemical dissolution processes such as calcium leaching. Two macroscopic numerical models are proposed as prototypes for hygrally and chemically induced degradation processes.

Chemically induced dissolution processes, such as calcium dissolution of cement cause an increase of porosity which may considerably affect the long-term durability of structures such as waste containments or pipelines exposed to water (Gérard 1996; Le Béllego et al. 2000). For this type of long-term degradation processes, the chemo-mechanical model by (Kuhl et al. 2000) based on the theory of mixtures (Bowen 1976) is proposed in Section 2. The evolution of mechanically and chemically induced porosities is controlled by internal parameters, which allow for the consideration of cyclic chemical loading.

Cracks induced by drying (Alvaredo 1994; Colina and Acker 2000) and the dependence of shrinkage, strength and stiffness of concrete on the moisture content (Pihlajavaara 1974) are examples for the considerable influence of moisture transport on the mechanical behavior of concrete. In turn, cracks, irrespective of its origin, promote the transport of moisture and render concrete structures even more vulnerable to external aggressive agents. For the modeling of these coupling effects, a hygro-mechanical model is formulated within the framework of thermomechanics of partially saturated porous media in the sense of Biot's theory (Biot 1941; Coussy 1995) in Section 3. A multisurface elastoplasticity-damage model formulated in terms of stresses and the capillary pressure allows for the description for shrinkage-induced cracks, of anisotropic stiffness degradation as well as of inelastic deformations.

2 MODEL FOR DISSOLUTION-RELATED DEGRADATION PROCESSES

As a particular example for chemical dissolution processes, the diffusion and dissolution of calcium and the interaction with damage mechanisms in cementitious materials is discussed in this section. Numerical models for this type of chemical degradation have been recently proposed by (Gérard 1996), (Gérard et al. 1998), (Pijaudier-Cabot et al. 1998), (Saetta et al. 1999) and (Le Béllego et al. 2000). In these papers two main interactions between both field problems are addressed: The dissolution of calcium in the cement paste leads to a decrease of mechanical material properties, namely the stiffness and strength. Vice versa, mechanical damage results in an increasing permeability for the calcium ions in the fluid phase.

Inspired by the work of (Ulm et al. 1999), in which an elasto-plastic material model was coupled with a model for the calcium leaching process within the theory of porous media, a formulation of coupled chemically and mechanically induced damage within the framework of the mixture theory by (Bowen 1976) was recently proposed by (Kuhl et al. 2000). The new aspects of this model are the consistent formulation of stiffness degradation and increasing conductivity resulting from both deterioration processes, the definition of an internal variable which allows for cyclic chemical loading and an equivalent formulation of the evolution equations for chemical and mechanical induced damage. Details of the numerical solution scheme by means of an implicit second order accurate time integration scheme and a hierarchical finite element formulation are proposed by (Kuhl et al. 2001).

2.1 Total porosity

The formulation of the total porosity ϕ, which is given by the sum of the initial porosity ϕ_0, the porosity due to matrix dissolution ϕ_c and the apparent mechanical porosity ϕ_m

$$\phi = \phi_0 + \phi_c + \phi_m, \tag{1}$$

allows for a consistent coupling between chemical and mechanical degradation in concrete. The chemical porosity ϕ_c is a function of the skeleton calcium concentration s in terms of the initial concentration s_0 and the average molar volume $\mathcal{M}/\rho$ of the skeleton. Since mechanical damage is restricted to the matrix material, the apparent mechanical porosity ϕ_m is defined by the volume fraction of the skeleton multiplied by the damage parameter d_m

$$\phi_c = \frac{\mathcal{M}}{\rho}\,(s_0 - s)\,, \quad \phi_m = (1 - \phi_0 - \phi_c)\, d_m. \tag{2}$$

2.2 Constitutive laws

The chemo-mechanical model is based on the potential energy of calcium ions Ψ_c and the strain energy of the skeleton deformation Ψ_m defined in the form

$$\Psi_c = \frac{\phi}{2}\, D_l\, \boldsymbol{\gamma} \cdot \boldsymbol{\gamma}\,, \quad \Psi_m = \frac{1-\phi}{2}\, \boldsymbol{\varepsilon} : \boldsymbol{C}_s : \boldsymbol{\varepsilon}. \tag{3}$$

$\boldsymbol{\gamma}$ is the negative gradient of the concentration field c and $\boldsymbol{\varepsilon}$ is the linearized strain tensor given by the symmetric part of the displacement gradient

$$\boldsymbol{\gamma} = -\nabla c\,, \quad \boldsymbol{\varepsilon} = \nabla^s \boldsymbol{u}. \tag{4}$$

D_l denotes the conductivity of the pure pore fluid and $\boldsymbol{C}_s$ is the isotropic elasticity tensor of the skeleton material. The macroscopic stress tensor $\boldsymbol{\sigma}$ and calcium mass flux vector $\boldsymbol{q}_c$ are determined by differentiation of the potential and the free energy function with respect to the $\boldsymbol{\varepsilon}$ and $\boldsymbol{\gamma}$, respectively, as

$$\boldsymbol{q}_c = \phi\, D_l\, \boldsymbol{\gamma}\,, \quad \boldsymbol{\sigma} = (1-\phi)\, \boldsymbol{C}_s : \boldsymbol{\varepsilon}. \tag{5}$$

2.3 Evolution of chemical and mechanical damage

The evolution of the porosity ϕ_c is described by means of the chemical degradation criterion formulated in terms of the calcium concentration and the chemical equilibrium threshold κ_c

$$\Phi_c = \kappa_c - c \leq 0. \tag{6}$$

According to the Kuhn-Tucker conditions and the consistency condition

$$\Phi_c \leq 0\,, \quad \dot{\kappa}_c \leq 0\,, \quad \Phi_c\, \dot{\kappa}_c = 0\,, \quad \dot{\Phi}_c\, \dot{\kappa}_c = 0 \tag{7}$$

the matrix dissolution process is connected with a decreasing chemical equilibrium calcium concentration ($\dot{\kappa}_c \leq 0$). The dissolution threshold κ_c is unchanged for $\Phi_c < 0$ and equal to the current calcium concentration of the pore fluid ($\kappa_c = c$) otherwise. The porosity due to chemical degradation ϕ_c is calculated by (2), where the change of the calcium concentration in the skeletons is calculated as function of the internal variable κ_c instead of the current concentration as proposed in the phenomenological equilibrium chemistry model by (Gérard 1996).

The evolution of the damage parameter κ_m is based on the damage criterion (Simo and Ju 1987)

$$\Phi_m = \eta(\boldsymbol{\varepsilon}) - \kappa_m \leq 0. \tag{8}$$

d_m, η and κ_m define the damage function, the equivalent strain function and the damage threshold. The Kuhn-Tucker loading/unloading conditions and the consistency condition are obtained as

$$\Phi_m \leq 0\,, \quad \dot{\kappa}_m \geq 0\,, \quad \Phi_m\, \dot{\kappa}_m = 0\,, \quad \dot{\Phi}_m\, \dot{\kappa}_m = 0. \tag{9}$$

(9) implies, that κ_m is unchanged for $\Phi_m < 0$ and given as $\kappa_m = \eta$ otherwise. The equivalent strain and the evolution of d_m as function of the internal variable κ_m can be calculated in a standard manner, see e.g. (Simo and Ju 1987).

2.4 Initial boundary value problem

The coupled system of calcium leaching and mechanical damage in porous cement pastes is characterized by the concentration field of calcium ions c and the displacement field $\boldsymbol{u}$ as primary variables and by a set of internal variables. The primary variables in the domain Ω are controlled by the conservation of the calcium ion mass contained in the pore space and the balance of linear momentum,

$$\begin{aligned} \operatorname{div} \boldsymbol{q}_c + [[\phi_0 + \phi_c]\ c\,]^{\cdot} + \dot{s} &= 0\,, \\ \operatorname{div} \boldsymbol{\sigma} &= 0. \end{aligned} \tag{10}$$

div$\boldsymbol{q}_c$ describes the spatial change of the mass flux vector, $[[\phi_0+\phi_c]c]^{\cdot}$ accounts for the change of the calcium mass due to the temporal change of the porosity and the concentration, $\dot{s}$ is the calcium mass production by matrix dissolution and div$\boldsymbol{\sigma}$ represents the spatial change of the macroscopic stress tensor. The system of differential equations (10) is accompanied by related boundary and initial conditions on the boundary Γ and in the domain Ω

$$\begin{array}{lll} c(t=0)=c_0^\star\,, & \boldsymbol{q}_c\cdot\boldsymbol{n}=q_c^\star\,, & c=c^\star, \\ \boldsymbol{u}(t=0)=\boldsymbol{u}_0^\star\,, & \boldsymbol{\sigma}\cdot\boldsymbol{n}=\boldsymbol{t}^\star\,, & \boldsymbol{u}=\boldsymbol{u}^\star, \end{array} \tag{11}$$

where $\boldsymbol{n}$ is the normal vector on the boundary surface, $q_c^\star$ is the calcium ion mass flux across the boundary, $c^\star$ is the prescribed concentration, $\boldsymbol{t}^\star$ is the traction vector and $\boldsymbol{u}^\star$ are prescribed displacements.

3 MODEL FOR MOISTURE-RELATED DEGRADATION PROCESSES

In the hygro-mechanical model, concrete is described on a macroscopic level within the framework of Biot's theory. A similar approach has been recently taken by (Carmeliet 1998; Carmeliet and Abeele 2000). Concrete is assumed to consist of the matrix material – a mixture of cement paste and the aggregates – and the pores, which are partially saturated by liquid water and an ideal mixture of water vapor and dry air. As a further simplification, the gas pressure within the pore space is assumed to be constant and uniform. Here, an anisotropic elastoplastic-damage material model for biaxially loaded concrete (Meschke et al. 1998) is employed.

3.1 State equations

Deformations are assumed to be small and consist of elastic and inelastic portions, i. e.

$$\boldsymbol{\varepsilon}=\boldsymbol{\varepsilon}^e+\boldsymbol{\varepsilon}^p, \qquad \phi=\phi_0+\phi^e+\phi^p, \tag{12}$$

with $\boldsymbol{\varepsilon}$ as the linearized strain tensor and ϕ as the total volume of pores. The function of free energy Ψ defining the poroplastic damage behavior of concrete is characterized by the dependence on external and internal variables

$$\begin{array}{rcl} \Psi & = & \Psi(\boldsymbol{\varepsilon},m_l,\boldsymbol{\varepsilon}^p,\phi^p,\boldsymbol{C},\alpha_R,\alpha_D) \\ & = & \frac{1}{2}(\boldsymbol{\varepsilon}-\boldsymbol{\varepsilon}^p):\boldsymbol{C}:(\boldsymbol{\varepsilon}-\boldsymbol{\varepsilon}^p) \\ & - & \left(\frac{m_l}{\rho_l}-\phi^p\right)Mb\boldsymbol{I}:(\boldsymbol{\varepsilon}-\boldsymbol{\varepsilon}^p), \end{array} \tag{13}$$

where $\boldsymbol{\varepsilon}$ and the moisture content m_l are external variables. The tensor of plastic strains $\boldsymbol{\varepsilon}^p$, the non-recoverable portion of the porosity ϕ^p, the degrading 4th-order drained stiffness tensor $\boldsymbol{C}$ and the variables α_R and α_D characterizing the pre- and postfailure behavior of concrete in tension (subscript R) and compression (subscript D) are internal variables. $\boldsymbol{I}$ denotes the second-order unit tensor and ρ_l is the density of the liquid.

From the entropy inequality, the state equations are obtained as

$$\boldsymbol{\sigma}=\frac{\partial\Psi}{\partial(\boldsymbol{\varepsilon}-\boldsymbol{\varepsilon}^p)}, p_l=\frac{\partial\Psi}{\partial(\frac{m_l}{\rho_l}-\phi^p)}, q_k=-\frac{\partial\Psi}{\partial\alpha_k}, \tag{14}$$

where the index k stands for R and D, respectively, $\boldsymbol{\sigma}$ is the stress tensor and p_l is the liquid pressure. q_R and q_D are stress-like variables which determine the damage-dependent size of the damage (f_R) and loading (f_D) surface in the stress space.

Inserting (13) into (14) and differentiation of the result provides the constitutive equations in differential form

$$\mathrm{d}\boldsymbol{\sigma}=\boldsymbol{C}:\,\mathrm{d}\boldsymbol{\varepsilon}^e+\mathrm{d}\boldsymbol{C}:\boldsymbol{\varepsilon}^e-b\,\mathrm{d}p_l\boldsymbol{I}, \tag{15}$$

$$\mathrm{d}p_l=M\left[-b\;\mathrm{dtr}\boldsymbol{\varepsilon}^e+\left(\frac{\mathrm{d}m_l}{\rho_l}-\mathrm{d}\phi^p\right)\right]. \tag{16}$$

Expressions for the hygro-mechanical coupling coefficients, namely the Biot coefficient b and the isotropic Biot modulus M, can be derived from comparing stress- and strain- quantities at the meso- and the macro-level (Coussy 1995; Cheng 1997; Shao 1998; Carmeliet 2000; Meschke and Grasberger 2001).

3.2 Material model for plane concrete

Biaxially loaded plain concrete is modeled within the framework of multisurface damage-plasticity theory (Meschke et al. 1998). Concrete cracking is represented numerically on the basis of the smeared crack concept (Rots and Blaauwendraad 1989). Anisotropic degradation of stiffness as well as inelastic deformations as a consequence of the opening of microcracks is accounted for. The ductile behavior of plain concrete subjected to predominantly compressive loading is phenomenologically described by means of an isotropic hardening plasticity model. In the model, both mechanisms are controlled by two threshold functions defining a region of admissible stress states in the space of „pseudo"-effective stresses $\boldsymbol{\sigma}'$

$$\mathbb{E}=\{\boldsymbol{\sigma}'\,|\,f_k(\boldsymbol{\sigma}',q_k)\le 0,\ \ k=1,2\}, \tag{17}$$

where the stress tensor $\boldsymbol{\sigma}'=\boldsymbol{\sigma}+b^p p_l\boldsymbol{I}$ represents the macroscopic counterpart to matrix-related microstresses (Meschke and Grasberger 2001) with the coefficient b^p as the plastic counterpart of the Biot coefficient b. An expression for b^p is derived in Section 3.3.

The index $k=1$ in (17) stands for an active cracking mechanism associated with the damage function $f_R(\boldsymbol{\sigma}',q_R)$ and $k=2$ represents an active hardening/softening mechanism in compression associated with the loading function $f_D(\boldsymbol{\sigma}',q_D)$. $q_1=q_R$ and $q_2=q_D$ are stress-like internal variables associated with f_R (f_D), respectively. They are defined as the thermodynamic forces conjugate to α_R and α_D according to $(14)_3$.

To account for the brittle material behavior of concrete in tension, the Rankine criterion is used. After crack initiation the residual stresses are gradually decreasing according to a hyperbolic softening law

$$q_R(\alpha_R) = f_{tu}\left[1-(1+\alpha_R/\alpha_{R,u})^{-2}\right]. \qquad (18)$$

The parameter $\alpha_{R,u}$ is adjusted to the specific fracture energy G_f of concrete in mode-I and to the length of the finite elements l_c according to the fracture energy concept for softening materials (Willam 1984). The ductile behavior of concrete subjected to compressive loading is described by a hardening/softening Drucker-Prager plasticity model. Details of the material model are found in (Meschke et al. 1998). The evolution equations of the tensor of plastic strains $\boldsymbol{\varepsilon}^p$ and of the elastic compliance moduli $\boldsymbol{D} = \boldsymbol{C}^{-1}$ are obtained from the postulate of stationarity of the dissipation functional as (Simo et al. 1993)

$$\begin{aligned} \dot{\boldsymbol{\varepsilon}}^p &= (1-\beta)\sum_{k=1}^{2}\dot{\gamma}_k\,\partial_{\boldsymbol{\sigma}'}f_k(\boldsymbol{\sigma}',q_k), \\ \dot{\boldsymbol{D}} &= \beta\sum_{k=1}^{m}\dot{\gamma}_k\frac{\partial_{\boldsymbol{\sigma}'}f_k(\boldsymbol{\sigma}',q_k)\,\partial_{\boldsymbol{\sigma}'}f_k^T(\boldsymbol{\sigma}',q_k)}{\partial_{\boldsymbol{\sigma}'}f_k^T(\boldsymbol{\sigma}',q_k)\boldsymbol{\sigma}'}, \end{aligned} \qquad (19)$$

together with the loading/unloading conditions

$$f_k \leq 0, \quad \dot{\gamma}_k \geq 0, \quad \dot{\gamma}_k f_k = 0. \qquad (20)$$

The parameter $0 \leq \beta \leq 1$ allows a simple partitioning of effects associated with inelastic slip processes, resulting in an increase of inelastic strains $\boldsymbol{\varepsilon}^p$ and deterioration of the microstructure, resulting in an increase of the compliance moduli $\boldsymbol{D}$.

3.3 Influence of moisture content on the material behavior

The concept of effective stresses (Fillunger 1936; von Terzaghi 1936) is a generally accepted approach in soil mechanics for the determination of stresses in the skeleton of fully saturated soils. In addition to the original proposal of (von Terzaghi 1936), several alternative suggestions for the definition of effective stresses exist (Lade and de Boer 1997). This concept has also been used for coupled hygro-mechanical models for cement-based materials (Coussy et al. 1998; Oshita and Tanabe 1999; Bary et al. 2000).

However, for the description of the fracture behavior of the matrix of partially saturated materials, a modification of the effective stress concept seems to be necessary. Following the notion of plastic effective stresses (Coussy 1995), an expression for a plastic effective stress has been suggested recently by (Burlion et al. 2000). In this paper, the effective stress was determined up to a material parameter, which was identified from experimental data. In what follows, the plastic effective stress tensor for saturated porous materials is also taken as the starting point for the determination of the coefficient b^p in (17) from relating stress quantities defined on the meso-level to respective homogenized quantities of the macro-level. The incremental macroscopic stress $\mathrm{d}\boldsymbol{\sigma}$ expressed in terms of the incremental solid matrix stress $\mathrm{d}\boldsymbol{\sigma}_s$ and the incremental liquid pressure $\mathrm{d}p_l$ yields

$$\begin{aligned} \mathrm{d}\boldsymbol{\sigma} &= (1-\phi)\,\mathrm{d}\boldsymbol{\sigma}_s - \phi S_l\;\mathrm{d}p_l\boldsymbol{I}, \\ &= \mathrm{d}\boldsymbol{\sigma}' - b^p\;\mathrm{d}p_l\boldsymbol{I}, \end{aligned} \qquad (21)$$

where S_l denotes the liquid saturation. (21) allows the interpretation of the incremental effective stress $\mathrm{d}\boldsymbol{\sigma}'$ as the part of the incremental macroscopic stress $\mathrm{d}\boldsymbol{\sigma}$ that is related to the incremental solid matrix stress $\mathrm{d}\boldsymbol{\sigma}_s$. From comparing (21) and (15), $\mathrm{d}\boldsymbol{\sigma}'$ and b_p can be identified as

$$\mathrm{d}\boldsymbol{\sigma}' = \boldsymbol{C} : \mathrm{d}\boldsymbol{\varepsilon}^e + \mathrm{d}\boldsymbol{C} : \boldsymbol{\varepsilon}^e - (b-b^p)\,\mathrm{d}p_l\boldsymbol{I}, \qquad (22)$$

and

$$b^p = \phi S_l. \qquad (23)$$

The coefficient $b - b^p$ can be interpreted as the part of the Biot coefficient b that is related to the nonlinear material behavior of the matrix material. In contrast to the classical effective stress concept the modified effective stress tensor defined in (22) allows for the description of shrinkage induced cracks and of the dependence of the material strength on the liquid saturation by means of material models formulated in the space of effective stresses. Hence, the usual engineering approach taken for the modeling of shrinkage cracks, using hygral strains associated to the moisture content, is not used here. Instead, in accordance with the underlying physical problem, (restrained) shrinkage is formulated as a purely stress-driven mechanism.

The plausibility of the expression (22) for the effective stress is evaluated by means of re-analyses of an extensive series of tests performed by (Pihlajavaara 1974) to study the effect of the equilibrium moisture content at different relative humidities of the surrounding air on the compressive and the flexural strength of various cement mortar beams (160 mm x 40 mm x 40mm). To this end the specimens were pre-cured for two years under sealed conditions prior to moisture conditioning of the specimens for three years in desiccators.

Since the Drucker-Prager model (Section 3.2) does not describe the concrete strength at triaxial states of stresses with sufficient accuracy, a more sophisticated formulation for the triaxial failure surface needed to be used for the re-analyses of these tests, since the capillary pressure induces a triaxial state of stress. Therefore the 5-Parameter failure sur-

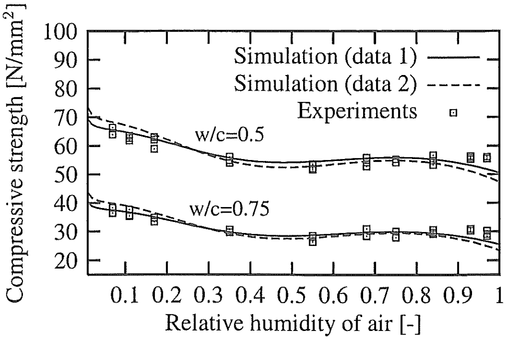

Figure 1: Dependence of the compressive strength of mature cement mortar on the equilibrium moisture content: Comparison of numerical simulation and experiments by (Pihlajavaara 1974)

face (Willam and Warnke 1974), characterized by two parabolic curves in the 0^o and 60^o meridians

$$\begin{aligned} \sigma_m &= a_0 + a_1\rho_t + a_2\rho_t^2, \\ \sigma_m &= b_0 + b_1\rho_c + b_2\rho_c^2, \end{aligned} \tag{24}$$

with $\sigma_m = I_1/3$ and $\rho = \sqrt{2J_2}$, was employed. Two sets of parameters given in (Schickert and Winkler 1977) and (Kotsovos and Newman 1979) were applied for comparison. In the analyses, the desorption isotherm of the cement mortar specimens and the initial porosity $\phi_0 = 0.24$ according to the data contained in (Pihlajavaara 1974) together with Kelvin's law were used. Two different types of cement mortar, characterized by water-cement ratios w/c=0.5 and w/c=0.75, respectively, were investigated.

Figure 1 illustrates a comparison of the experimental determined compressive strength and the associated numerical simulations for different relative humidities, using the material parameters of (Schickert and Winkler 1977) (data 1) and (Kotsovos and Newman 1979) (data 2). A good quantitative correlation of numerical and experimental results is observed for the compression tests. According to the model, at relative humidities larger than 85%, the strength decreases slightly. In the experiments, at high levels of relative humidity, the strength increases beyond 85 % up to a level of approximately 95%. At higher humidity levels, also in the experimental data, in particular for w/c=0.75 (Figure 1), a slight decrease of the compressive strength is observed.

3.4 Initial boundary value problem

The coupled system of mechanical deformation and moisture transport is characterized by the displacement field $\boldsymbol{u}$ and the capillary pressure p_c together with a set of internal variables. The primary variables in the domain Ω are controlled by the balance of linear momentum and by the conservation of the liquid mass in the pore space analogous to Section 2.4 as

$$\begin{aligned} \text{div}\boldsymbol{q}_l + \dot{m}_l &= 0, \\ \text{div}\boldsymbol{\sigma} &= 0. \end{aligned} \tag{25}$$

In (25), div$\boldsymbol{q}_l$ describes the spatial change of the liquid mass flux vector and $\dot{m}_l$ accounts for the change of the liquid saturation. The related boundary and initial conditions on the boundary Γ are defined as

$$\boldsymbol{\sigma}\cdot\boldsymbol{n} = \boldsymbol{t}^\star, \;\; \boldsymbol{q}_l\cdot\boldsymbol{n} = q_l^\star, \;\; \boldsymbol{u} = \boldsymbol{u}^\star, \;\; p_c = p_c^\star, \tag{26}$$

and in the domain Ω

$$\boldsymbol{u}(t=0) = \boldsymbol{u}_0^\star, \quad p_c(t=0) = p_{c,0}^\star. \tag{27}$$

In (26), $q_l^\star$ is the liquid mass flux across the boundary and $p_c^\star$ is the prescribed capillary pressure.

4 NUMERICAL EXAMPLE: BASE-RESTRAINED CONCRETE WALL

Restrained shrinkage is one of the major causes of damage in concrete structures. In order to demonstrate the capability of the hygro-mechanical model to reproduce shrinkage induced cracks, a numerical simulation of a concrete wall subjected to drying, but

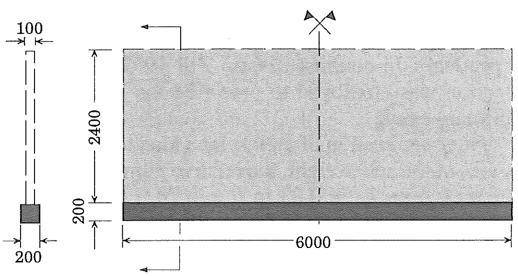

Figure 2: Numerical example: Geometry of the concrete wall (van Zijl 1999) (Dimensions in [mm])

restrained at the base by a non-shrinking foundation, is described in this section. A similar numerical example has been investigated by (van Zijl et al. 1998; van Zijl 1999), who analysed masonry walls subjected to restrained shrinkage.

Figure 2 shows the geometry of the investigated concrete wall. The following material parameters were assumed: Young's modulus $E = 43600$ N/mm^2, Poisson's ratio $\nu = 0.2$, uniaxial tensile strength $f_{tu} = 4.0$ N/mm^2, uniaxial compressive strength $f_{cu} = 63.4$ N/mm^2, fracture energy in tension $G_f = 0.1195$ N/mm, fracture energy in compression $G_c = 5.9750$ N/mm and $\beta = 0.20$. The following relationship between the capillary pressure and the liquid saturation was used (Baroghel-Bouny et al. 1999):

$$p_c(S_l) = 18.62\left[S_l^{-2.27} - 1\right]^{1-1/2.27}. \tag{28}$$

Furthermore, Kelvin's law gives the relation between p_c and the relative humidity h. The initial pore humid-

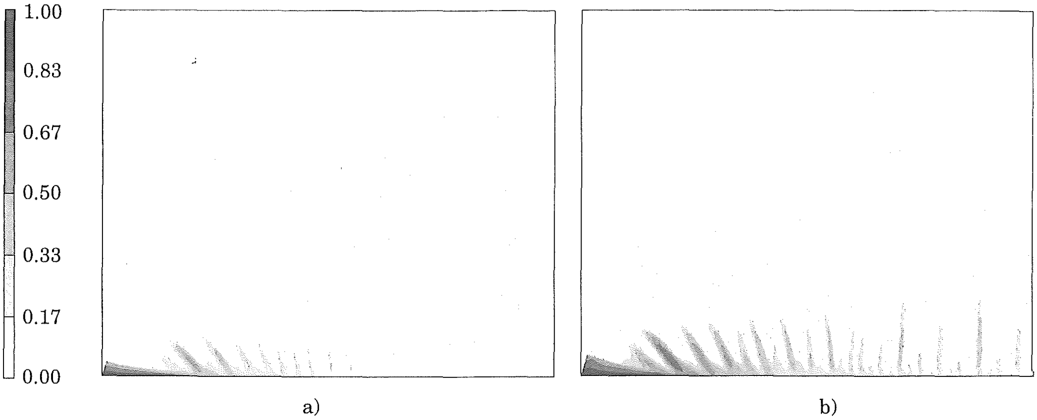

Figure 3: Numerical example: Calculated distribution of the scalar damage measure d for different states of drying a) $h = 0.80$ b) $h = 0.70$

ity was specified as $h_0 = 0.93$ and the initial porosity as $\phi_0 = 0.20$.

So far, the FE-implementation of the model is restricted to 2D problems. A 2D analysis of one half of the concrete wall, using 8910 four-noded plane stress elements, was performed. A uniform humidity was assumed within the wall. This simplified assumption is justified by the large surface exposed to the surrounding air and the small thickness of the wall, respectively. In contrast to (van Zijl 1999), no imperfection was employed to prescribe the location of a primary crack.

After application of an in-plane load taken as eight times of the self-weight, the relative humidity was decreased from $h_0 = 0.93$ to $h = 0.70$. Figure 3 illustrates the distribution of the scalar damage measure d due to the uniform drying of the concrete wall at $h = 0.80$ and $h = 0.70$. A horizontal crack opens already at $h = 0.90$. At $h = 0.80$, skew cracks start to open in the vicinity of the crack process zone of the horizontal crack with an inclination of 45^o with respect to the base line. As the drying proceeds, these skew cracks are further opening, while additional cracks start to open along the bottom of the slab, characterized by a larger angle approaching an angle of 90^o as the cracks approach the center of the slab.

5 SUMMARY AND CONCLUSIONS

In the paper, two numerical strategies for durability-oriented numerical analyses were described. One class of models was developed to describe the coupled effects of calcium leaching and of mechanical loading on the long term behavior of concrete structures subjected to water. The typical time scale of the degrading effect is in the range of several hundred years. Full coupling between calcium dissolution and mechanical induced damage was accomplished by the definition of the total porosity as the sum of the initial porosity, the porosity caused by the calcium dissolution and the apparent porosity due to mechanical loading. A second class of model was developed to account for the effect of moisture on the material behavior of concrete. The time scale of these processes is typically in the range of several hundred days. A strength criterion defined in the space of modified effective stresses allows for the prediction of shrinkage induced cracks in the framework of Biot's theory. Furthermore, it was shown, that the dependence of the compressive strength on the relative humidity could be well replicated by the proposed hygro-mechanical model.

ACKNOWLEDGMENT

Financial support was provided by the German National Science Foundation (DFG) in the framework of project A9 of the collaborative research center SFB 398 and through the graduate program *Computational Structural Dynamics*. This support is gratefully acknowledged.

REFERENCES

Alvaredo, A. (1994). Drying shrinkage and crack formation. Technical Report 5, Building Materials Reports, Aedificatio, Freiburg.

Baroghel-Bouny, V., M. Mainguy, T. Lassabatère, and O. Coussy (1999). Characterization and identification of equilibrium and transfer moisture properties for ordinary and high-performance cementitious materials. *Cement and Concrete Research 29*, 1225–1238.

Bary, B., J.-P. Bournazel, and E. Bourdarot (2000). Poro-damage approach applied to hydro-fracture analysis of concrete. *Journal of Engineering Mechanics 126*, 937–943.

Biot, M. (1941). General theory of three-dimensional consolidation. *Journal of Applied Physics 12*, 155–165.

Bowen, R. (1976). Theory of mixtures. In *Continuum Physics, Vol.3*, pp. 1–127. Academic Press, New York.

Burlion, N., F. Bourgeois, and J. Shao (2000). Coupling damage - drying shrinkage: experimental study and modelling. In V. Baroghel-Bouny and P.-C. Aïtcin (Eds.), *Proceedings of the International RILEM Workshop on Shrinkage of Concrete*, Number 17 in RILEM Proceedings.

Carmeliet, J. (1998). A poroviscoelastic damage model for hygromechanical damage processes in unsaturated porous media. In R. de Borst, N. Bićanić, H. Mang, and G. Meschke (Eds.), *Computational Modelling of Concrete Structures*, pp. 559–566. Balkema, Rotterdam.

Carmeliet, J. (2000). Poroelastic damage model for unsaturated porous media: Part 1: Constitutive modelling. *International Journal for Solids and Structures*. submitted.

Carmeliet, J. and K. V. D. Abeele (2000). Poromechanical modelling of shrinkage and damage processes in unsaturated porous media. In V. Baroghel-Bouny and P.-C. Aïtcin (Eds.), *Proceedings of the International RILEM Workshop on Shrinkage of Concrete*, Number 17 in RILEM Proceedings.

Cheng, A.-D. (1997). Material coefficients of anisotropic poroelasticity. *International Journal of Rock Mechanics and Mining Sciences 34*, 199–205.

Colina, H. and P. Acker (2000). Drying cracks: Kinematics and scale laws. *Materials and Structures 33*, 101–107.

Coussy, O. (1995). *Mechanics of porous continua*. Chichester: John Wiley & Sons.

Coussy, O., R. Eymard, and T. Lassabatère (1998). Constitutive modeling of unsaturated drying deformable materials. *Journal of Engineering Mechanics 124*(6), 658–667.

Fillunger, P. (1936). *Erdbaumechanik?* Wien.

Gérard, B. (1996). *Contribution des couplages mécanique-chimie-transfert dans la tenue a long terme des ouvrages de stockage de déchets radioactifs*. Ph. D. thesis, E.N.S. de Cachan.

Gérard, B., G. Pijaudier-Cabot, and C. Laborderie (1998). Coupled diffusion-damage modelling and the implications on failure due to strain localisation. *International Journal for Solids and Structures 35*, 4107–4120.

Kotsovos, M. and J. Newman (1979). A mathematical description of the deformational behavior of concrete under complex loading. *Magazine of Concrete Research 31*, 77–90.

Kuhl, D., F. Bangert, and G. Meschke (2000). An extension of damage theory to coupled chemo-mechanical processes. European Congress on Computational Methods in Applied Sciences and Engineering, 11.-14. September 2000, Barcelona, Spain.

Kuhl, D., F. Bangert, and G. Meschke (2001). Simulation of coupled chemo-mechanical deterioration of cementious materials. *International Journal for Solids and Structures*. submitted.

Lade, P. and R. de Boer (1997). The concept of effective stress for soil, concrete and rock. *Géotechnique 47*, 61–78.

Le Béllego, C., B. Gérard, and G. Pijaudier-Carbot (2000). Chemo-mechanical effects in mortar beams subjected to water hydrolysis. *Journal of Engineering Mechanics (ASCE) 126*(3), 266–272.

Meschke, G. and S. Grasberger (2001). Numerical modeling of coupled hygro-mechanical degradation of cementitious materials. *Journal of Engineering Mechanics (ASCE)*. submitted.

Meschke, G., R. Lackner, and H. Mang (1998). An anisotropic elastoplastic-damage model for plain concrete. *International Journal for Numerical Methods in Engineering 42*, 703–727.

Oshita, H. and T. Tanabe (1999). Measurement of pore water pressure in concrete and fracturing concrete by pore pressure. In G. Pijaudier-Cabot, Z. Bittnar, and B. Gérard (Eds.), *Mechanics of Quasi-Brittle Materials and Structures*, pp. 233–268. Hermes, Paris.

Pihlajavaara, S. (1974). A review of some of the main results of a research on the ageing phenomena of concrete: Effect of moisture conditions on strength, shrinkage and creep of mature concrete. *Cement and Concrete Research 4*, 761–771.

Pijaudier-Cabot, B., B. Gérard, N. Burlion, and L. Molez (1998). Localisation of damage in quasi-brittle materials and influence of chemically activated damage. In R. de Borst and E. van der Giessen (Eds.), *Material instabilities in solids*, pp. 442–456. John Wiley & Sons, Chichester.

Rots, J. and J. Blaauwendraad (1989). Crack models for concrete: Discrete or smeared? Fixed, multi-directional or rotating? *Heron 34*.

Saetta, A., R. Scotto, and R. Vitaliani (1999). Coupled enviromental-mechanical damage model of RC structures. *Journal of Engineering Mechanics (ASCE) 125*(8), 930–940.

Schickert, G. and H. Winkler (1977). Results of tests concerning strength and strain of concrete subjected to multiaxial compressive stresses. Technical Report 277, Deutscher Ausschuß für Stahlbeton.

Shao, J. (1998). Poroelastic behaviour of brittle rock materials with anisotropic damage. *Mechanics of Materials 30*, 41–53.

Simo, J. and J. Ju (1987). Strain and stress-based continuum damage model - I. formulation. *International Journal for Solids and Structures 23*(7), 821–840.

Simo, J., J. Oliver, and F. Armero (1993). An analysis of strong discontinuities induced by strain softening in rate-independent inelastic solids. *Computational Mechanics 12*, 277–296.

Ulm, F.-J., J.-M. Torrenti, and F. Adenot (1999). Chemoporoplasticity of calcium leaching in concrete. *Journal of Engineering Mechanics (ASCE) 125*(10), 1200–1211.

van Zijl, G. (1999). *Computational Modelling of Masonry Creep and Shrinkage*. Ph. D. thesis, TU Delft.

van Zijl, G., R. de Borst, and J. Rots (1998). FE analysis of the interaction between moisture migration, creep, shrinkage and cracking. In R. de Borst, N. Bićanić, H. Mang, and G. Meschke (Eds.), *Computational Modelling of Concrete Structures*, pp. 505–511. Balkema, Rotterdam.

von Terzaghi, K. (1936). The shearing resistance of saturated soils and the angle between the planes of shear. In *First Int. Conf. Soil Mech.*, Volume 1, pp. 54–56. Harvard University.

Willam, K. (1984). Experimental and computational aspects of concrete failure. In F. Damjanić (Ed.), *Computer aided analysis and design of concrete failure*, pp. 33–70. Pineridge Press, Swansea.

Willam, K. and E. Warnke (1974). Constitutive model for the triaxial behaviour of concrete. In *IABSE Seminar on Concrete Structures Subjected to Triaxial Stresses*, Volume 3, Bergamo.